15 Singer, R., and Araújo, I.J.S., Litter decomposition and ectomycorrhiza in an amzonian forest. Acta amazon. *9* (1979) 25–41.
16 Vanzolini, P.E., and Gomes, N., Notes on the ecology and growth of amazonian Caimans (Crocodylia, Alligatoridae). Papéis avulsos de Zool., São Paulo *32* (1979) 205–216.
17 Vanzolini, P.E., A quasi-historical approach to the natural history of the differentiation of reptiles in tropical, geographic isolates. Papéis avulsos de Zool., São Paulo *34* (1981) 189–204.
18 Vanzolini, P.E., and Williams, E.E., The vanishing refuge: a mechanism for ecogeographic speciation. Papéis avulsos Zool., São Paulo *34* (1981) 251–255.
19 Walker, I., The physical dimension and biological meaning of the coefficents in the Volterra competition equations and their consequences for the possibility of coexistence. Acta biotheor. *32* (1983) 93–122.
20 Walker, I., The Volterra competition equations with resource-independent growth coefficients and discussion on their biological and biophysical implications. Acta biotheor. *33* (1984) 253–270.

0014-4754/87/0287-04$1.50 + 0.20/0

Short Communications

Prey localization by surface wave ray-tracing: Fish track bugs like oceanographers track storms

R.H. Käse* and H. Bleckmann+

Neurobiology Unit, Scripps Institution of Oceanography, and Department of Neurosciences, School of Medicine, University of California, San Diego, La Jolla (California 92093, USA), 26 June 1986

Summary. Surface-feeding fish accurately determine direction and distance to the center of a concentric wave stimulus, even if only a single, short lasting wave train is presented[1,2]. It has been suggested that one cue used by these fish to localize the wave center is the distance dependent frequency modulation of the initial part of a wave stimulus[3,4]. Here we show how the distance information contained in the fractional frequency change of a capillary wave group can be decoded. We suggest that wave source localization in surface-feeding fish in part is based on a principal similar to that used by oceanographers to track storms by the frequency change of forerunners of swell.
Key words. Surface-feeding fish; water surface waves; lateral line; distance determination; ray-tracing.

Surface-feeding fish prey on terrestrial insects trapped at the water surface. These fish detect and localize their insect prey with aid of water surface waves generated by the preys struggling[1,2]. The receptors involved are mechanosensitive lateral line organs located at the fish's head and back[5]. Visually deprived surface-feeding fish can be conditioned to respond to wave stimuli (called clicks) generated by a single air blow or by dipping a small rod once into the water. Even if a single click is presented these fish determine the direction and distance to the wave source up to 10–15 cm precisely[1,2]. Because a click lasts shorter than the time needed for the fish to reach the wave source, surface-feeding fish are able to localize the center of a concentric wave stimulus under open loop conditions, i.e. these fish can localize a remembered wave target.

Water surface waves as caused by prey objects of surface-dwelling predators are in the mm to cm (5–140 Hz) wavelength range[6]. An isolated strongly localized initial disturbance of the water surface can be thought of as the combination of large number of sinusoidal oscillations (Fourier-components[7]) with different wave lengths (λ) and frequencies (ω, where ω is $2\pi f$). In low-frequency ($\ll$ 13 Hz) waves gravity is the most important restoring agent. Gravity waves in deep water have normal dispersion characteristics, i.e. the longer waves travel faster than the shorter waves. In capillary waves ($\gg$ 13 Hz) the most important restoring force is surface tension. Capillary waves are abnormally dispersive, i.e. the shorter waves are faster than the longer waves. In deep water (water depth $\gg \lambda$) the following equation describes the dispersion relationship of surface waves[7]

$$c_{ph}^2 \equiv \frac{\omega^2}{K^2} = \left(g + \frac{T \cdot K^2}{\varrho}\right) K^{-1} \qquad (1)$$

where g is the gravitational acceleration, K is the wave number ($2\pi/\lambda$), ϱ is the density of the water, T is the coefficient of surface tension, and c_{ph} is the phase velocity. For typical parameters ($g = 981$ cm/s^2 and $T/\varrho = 72$ cm^3/s^2) the minimal phase velocity of water surface waves is 23.1 cm/s at a wavelength of about 1.7 cm (corresponding to a frequency of 13 Hz) (fig. 1). Consequently in the frequency range 5–140 Hz, waves of 1.7 cm length form the rear portion of a wave packet.

Wave energy propagates with group velocity (c_g) which is defined as the rate of change of frequency with wave number[7]

$$c_g \equiv d\omega/dK = c_{ph} - \lambda\,(dc_{ph}/d\lambda) \qquad (2)$$

Group velocity is slower than phase velocity in normal dispersion ($dc_{ph}/d\lambda > 0$) and faster than phase velocity in abnormal dispersion ($dc_{ph}/d\lambda < 0$)[7]. After traveling a certain distance, a dispersive wave group consists of a band of different wavelengths and frequencies. Locally a wavelength can be defined by the crest to crest distance, but due to dispersion the distance of successive crests differs by a small amount. These differences reflect both the distance dependent frequency modulation of the wave group and the speed with which the wave packet spreads in space.

When surface-feeding fish are confronted with a computer controlled wave stimulus which is generated at 7 cm but simulates the frequency modulation of a click at 15 cm, they swim on average 4–6 cm beyond the wave source (fig. 2). Therefore it has been suggested that these fish use the frequency modulation of the first few wave cycles of a capillary wave train to determine prey distance D[3,4]. There is, however, a variation in frequency modulation at a given source distance, if different types of wave generators are used[3]. Because the observed variations in frequency modulation were small, it was assumed that they may cause some uncertainty or variability in the orientation response of surface-feeding fish[3]. Also, to date, it has not been shown how the information contained in the frequency modulation of a wave stimulus can be decoded. Here we demonstrate that the wave source distance D unequivocally can be calculated if both the local frequency of the initial part of a wave stimulus and the fractional frequency change around this local frequency are

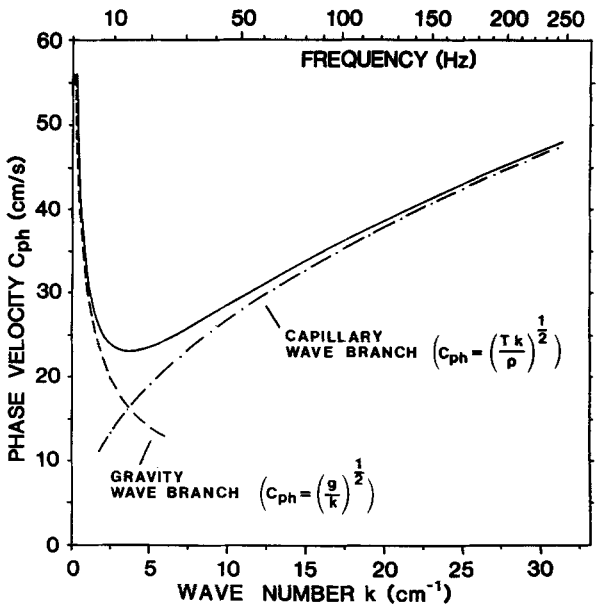

Figure 1. The wave speed c_{ph} for ripples on deep water (full line). Asymptotes for pure capillary waves (dashed-dotted) and gravity waves (dashed) are also shown. Transition occurs around a frequency of 13 Hz, where phase velocity is minimal.

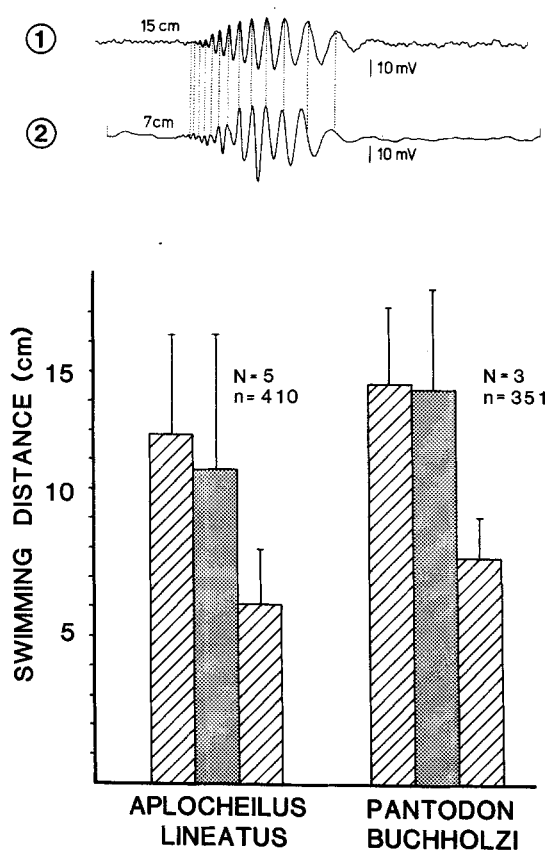

Figure 2. Mean swimming distance of visually deprived surface-feeding fish *Aplocheilus lineatus* and *Pantodon buchholzi* towards the wave source after presenting a surface wave stimulus. For each species from left to right: responses to a click at 15 ± 1.5 cm source distance, to a wave stimulus at 7 ± 0.5 cm simulating a click at 15 cm, and to a click at 7 ± 0.5 cm source distance. In all cases the middle of the fish's head (top view) served as reference. At top of the figure: (1) Wave stimulus caused by a click at 15 cm source distance and (2) simulation of this stimulus at 7 cm source distance. N, number of fish; n, number of experiments (after (6)).

known. The mechanism we present is independent of the upper frequency limit, the frequency range, the absolute frequency modulation, and the amplitude of the initial part of a capillary wave stimulus.

An isolated wave packet generated by an initial spatially symmetric disturbance in D=0 and having the Fourier-amplitude spectrum A(K) at time t = 0 has the approximate space-time distribution[7]

$$a(D,t)=\frac{A(K_s)e^{-\nu K_s^2 t}}{[K_s D/c_g'(K_s)/t]^{1/2}}\cdot\cos(K_s(D-c_{ph}\cdot t)) \qquad (3)$$

where v is the kinematic viscosity, the prime denotes a derivative with respect to wave a number, and K_s is the wave number of stationary phase corresponding to the capillary wave root of the ray equation

$$D=c_g(K_s)\cdot t \qquad (4)$$

Eqs 3 and 4 describe the space-time distribution of a wave train in terms of a slowly varying amplitude function and a rapidly oscillating trigonometric function. The exponential accounts for the damping of the wave stimulus by frictional effects, and the denominator represents the effect of energy conservation due to the geometric and dispersive spreading. Both frequency and wave number K_s are slowly varying functions of space and time. In a space-time diagram the group velocity of a given part of the wave stimulus is defined by the slope of a straight line (a ray) drawn through the wave's origin (fig. 3). The capillary wave groups caused by an initial disturbance of a Gaussian shape and a diameter of 3 mm are shown at a distance of 5 cm, 10 cm, and 15 cm from the source calculated from eqs 3 and 4. As can be seen, the high-frequency waves travel ahead of the disturbance with lower frequencies continuously arriving at later times.

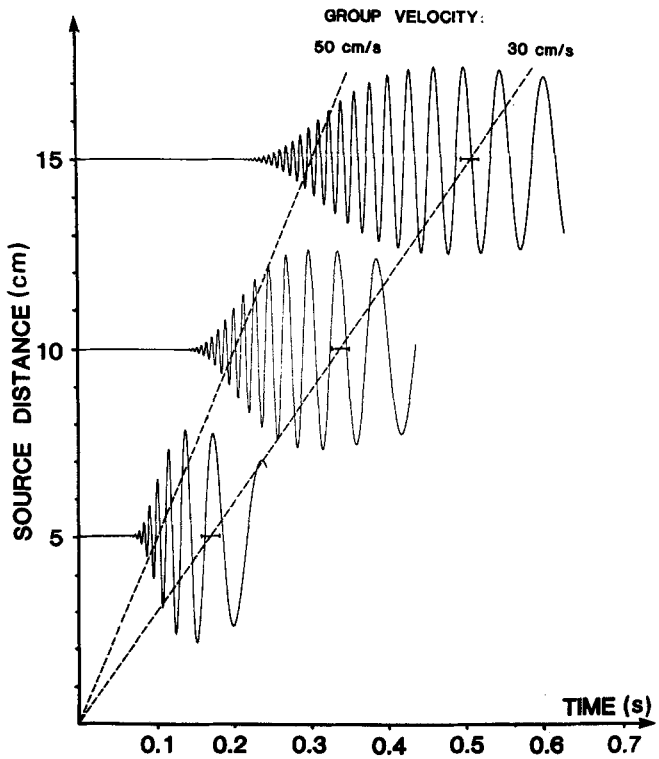

Figure 3. Time-space diagram of a dispersive capillary wave train shown at 5 cm, 10 cm, and 15 cm distance from the source. The two dotted lines (rays) connect points of equal frequency as is indicated by the 3 bars. Amplitudes are exaggerated for better visualization according to a factor $(k_s D_0)^{\frac{1}{2}}\cdot t/t_0$ with D_0 = 1 cm and t_0 = 1 s.

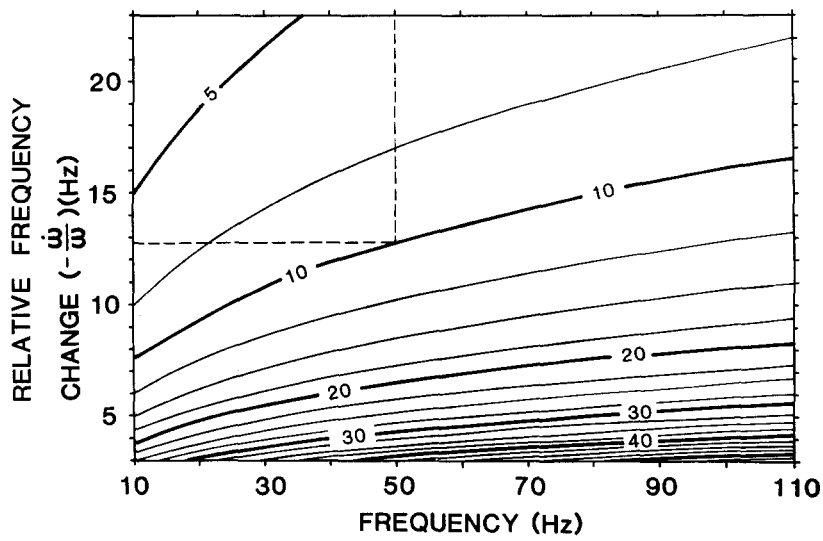

Figure 4. Range contours as function of relative frequency change and local frequency. For example, a wave stimulus with a local frequency of 50 Hz and a relative frequency change of 12.8 Hz has traveled a distance of 10 cm as indicated by the intersection of the dashed lines.

Along a wave ray frequency is conserved (as indicated by the bars in fig. 3) whereas the phase changes continuously. Since all rays intersect at the wave origin it is possible to locate the stimulus source by constructing any 2 rays. This general method has been used by oceanographers for tracking storms by forerunners of swells, using the gravity branch of the dispersion relationship[8–10]. Applying this technique, Snodgrass et al.[10] were able to trace swells generated in the southern hemisphere across the whole Pacific Ocean.

Since the frequency is conserved along a wave ray, only two measurements of the group velocity are necessary to determine the two unknowns in the system, namely the elapsed time (t) which has passed since the generation of the wave packet and the source distance D. At a certain distance the slope of two different rays at times t_1, t_2 are the group velocities c_{g1}, c_{g2}. Because the time of wave generation is not known eq. 4 written at times t_1, t_2 can be combined to

$$D = (t_2 - t_1)/((1/c_{g2}) - (1/c_{g1})) \tag{5}$$

where the absolute time is eliminated. For small time changes the observed frequencies differ only by a small amount, say $\Delta\omega$. Thus $c_{g2}(\omega) = c_{g1}(\omega + \Delta\omega)$. Taylor series expansion to first order $(c_{g1}(\omega + \Delta\omega) \approx c_{g1}(\omega) + (dc_{g1}/d\omega)\Delta\omega)$ yields

$$D = c_{g1} \frac{-(t_2 - t_1)}{\Delta\omega} \Big/ \left(\frac{1}{c_{g1}} \cdot \frac{dc_{g1}}{d\omega} \right) \tag{6}$$

In the infinitesimal limit $(t_2 - t_1 = \Delta t \to 0$, and $\Delta t/\Delta\omega \to 1/(d\omega/dt)) = 1/\dot{\omega}$ eq. 7 follows after using group velocity of eq. 2.

$$D = -\frac{9}{2} c_{ph} \cdot \frac{\omega}{\dot{\omega}} \tag{7}$$

Dotted variables denote to derivatives with respect to time. Figure 4 displays the range contours as a function of the local frequency and the relative frequency change within a wave group. For example a stimulus with a local frequency of 50 Hz and a relative frequency change of 12.8 Hz around this local frequency has traveled a distance of 10 cm (dashed lines in fig. 4). As can be seen the decoding of distance information with aid of ray-tracing is independent of stimulus amplitude, frequency range, upper frequency limit, and absolute frequency modulation. As long as the initial part of a wave stimulus contains more than one frequency component the extraction of distance information is solely a question of the sensory and neural capabilities of the wave receiver. Figure 4 also shows that the relative frequency change $-\frac{\dot{\omega}}{\omega}$ is larger close to the wave source and that the distance between the range contours decreases constantly with increasing source distance. This indicates that animals which use $-\frac{\dot{\omega}}{\omega}$ to determine D will make an increasing absolute localization error with increasing source distance. This fits well with the orientation behavior observed in surface-feeding fish[1,2].

That surface-feeding fish have the sensory and neural capabilities to perform the localizing mechanism just proposed is very likely. The extreme sensitivity of the head lateral line system to capillary waves (down to 0.04–0.007 μm displacement at 100–150 Hz[11–13]) probably allows these fish to get the information encoded in the initial, weak-amplitude high-frequency part of a wave train. In the relevant frequency range 10–150 Hz surface-feeding fish can discriminate water wave frequencies to a resolution of at least 10%[14]. Thus these fish are probably able to measure both, the local frequency and the frequency modulation (fig. 2) of the initial part of a wave stimulus. We suggest that evolution has provided surface-feeding fish with a localizing mechanism based on a simple physical principle which has been used by oceanographers to track storms at sea.

Acknowledgments. We thank Drs T. H. Bullock, W. Heiligenberg, W. H. Munk, and L. Washburn for critically reading early drafts of the manuscript. L. Washburn in addition deserves our thanks for improving our English. Supported by grants of the DFG to H. Bleckmann (Bl 242/1-1), R. H. Käse (Kä 399/2-1), and NSF and NIH grants to T. H. Bullock.

* Present address: Institut für Meereskunde an der Universität Kiel, 2300 Kiel, Federal Republic of Germany.
+ To whom correspondence should be addressed.

1 Schwartz, E., Z. vergl. Physiol. *50* (1965) 55.
2 Schwartz, E., Z. vergl. Physiol. *74* (1971) 64.
3 Bleckmann, H., and Schwartz, E., J. comp. Physiol. *145* (1982) 331.
4 Hoin-Radkovski, I., Bleckmann, H., and Schwartz, E., Anim. Behav. *32* (1984) 840.
5 Schwartz, E., Z. Morph. Ökol. Tiere *67* (1970) 40.
6 Lang, H. H., Behav. Ecol. Sociobiol. *6* (1980) 233.
7 Lighthill, J., Waves in Fluids. Cambridge Univ. Press, London 1978.
8 Munk,. W. H., J. Met. *4* (1947) 45.
9 Barber, B. F., and Ursell, F., Phil. Trans. R. Soc. *240* (1948) 527.
10 Snodgrass, F. E., Groves, G. W., Hasselmann, K. F., Miller, G. R., Munk, W. H., and Powers, W. H., Phil. Trans. R. Soc. *259* (1966) 431.
11 Müller, U., Thesis, Universität Giessen (1984).

12 Bleckmann, H., J. comp. Physiol. *145* (1980) 163.
13 Bleckmann, H., and Topp, G., Naturwissenschaften *67* (1981) 624.
14 Bleckmann, H., Waldner, I., and Schwartz, E. J. comp. Physiol. *143* (1981) 485.

0014-4754/87/0290-04$1.50 + 0.20/0

Circadian pacemaker does not arrest in deep hibernation. Evidence for desynchronization from the light cycle

H. Pohl

Max-Planck-Institut für Verhaltensphysiologie, Vogelwarte, D-8138 Andechs (Federal Republic of Germany), 9 April 1986

Summary. A freerunning rhythm of locomotor activity was observed between hibernation bouts in Turkish hamsters *(Mesocricetus brandti)* kept in 10L:14D light-dark cycles at 10 ± 1 °C. The data further indicate an influence of natural hypothermia upon the circadian system and its ability to entrain to light-dark cycles.
Key words. Hibernation; circadian rhythms; entrainment; light-dark cycle; desynchronization; Turkish hamster.

Twenty-five years ago evidence was presented that the circadian clock continues to run in hibernating mammals[1,2]. In the common dormouse *(Glis glis)* a circadian rhythm of locomotor activity was shown to persist throughout the hibernation season (for about 280 days) in constant darkness and cold[3]. Freerunning rhythms of heterothermy were subsequently observed in the garden dormouse *(Eliomys quercinus)*[4] and in the western jumping mouse *(Zapus princeps)*[5]. The ability of these rhythms to entrain to 24-h light-dark (LD) cycles was shown for both species of dormice[3,4]. Recently, Vaněček and co-workers[6] have presented data which suggest that the circadian pacemaker which drives the rhythm of melatonin formation in the pineal is arrested during hibernation bouts in the Syrian hamster *(Mesocricetus auratus)*. New data from the closely related Turkish hamster *(M. brandti)*, however, show that a circadian rhythm of activity can persist through bouts of hibernation up to about 100 h.

The presented data derive from an experiment in which 7 Turkish hamsters (4 ♂; 3 ♀) were held under constant 10L:14D light-dark cycles (150:0.02 lx) for 18 months beginning from the middle of October 1984. The hamsters were born during the previous summer and were maintained under natural daylengths. Ambient temperature was 19 ± 1 °C before 20 December and 10 ± 1 °C thereafter. Activity was continuously recorded by a photocell and an infrared light source in the middle of the cage. Whenever the animal crossed the light beam, a contact was closed on an event-recorder channel. In addition, the sum of all impulses was recorded in 2-min intervals on magnetic disk (Kräussling system) for further computer processing. Food pellets (Altromin) and tap water were given ad libitum.

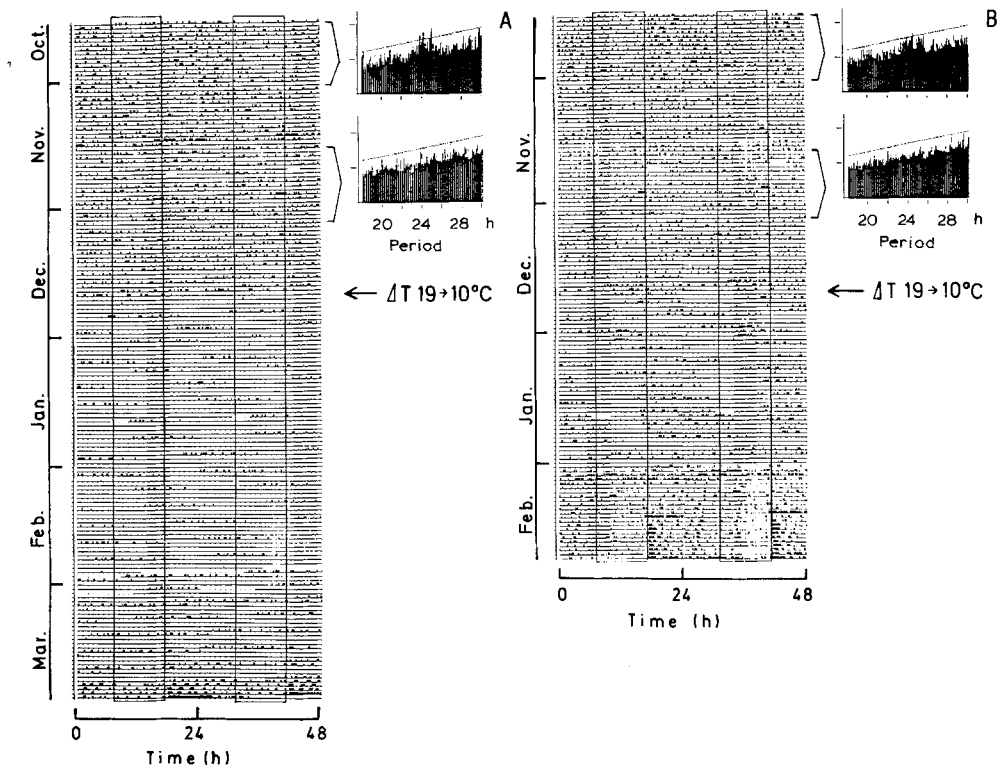

Original recordings of locomotor activity of 2 Turkish hamsters during the hibernation season. The animals were exposed to LD 10:14 (L indicated by frame). Records of successive days are plotted underneath each other on a 48-h scale. On 20 December, ambient temperature was changed from 19 to 10 °C. On the right margin of each record, chi-square periodograms are shown for sections indicated by brackets. Vertical lines reaching at or above the inclined line indicate significant values. White spaces on the records indicate recording failures.